# Catalysis Science & Technology

Accepted Manuscript

ROYAL SOCIETY OF CHEMISTRY

www.rsc.org/catalysis

Journal Name RSCPublishing

COMMUNICATION

Cite this: DOI: 10.1039/x0xx00000x

# Catalytic dehydrofluorination of 1, 1, 1, 2-tetrafluoroethane to synthesize trifluoroethylene over the modified NiO/$Al_2O_3$ catalyst

Wenzhi Jia, Min Liu, Xuewei Lang, Chao Hu, Junhui Li and Zhirong Zhu*[a]

Received 00th January 2012,
Accepted 00th January 2012

DOI: 10.1039/x0xx00000x

www.rsc.org/

**A promising fluorinated NiO/$Al_2O_3$ catalyst to synthesize trifluoroethylene through catalytic dehydrofluorination of $CF_3CFH_2$ was prepared, and the relationship between the Lewis acid sites and activity was investigated. As a result, the conversion of $CF_3CFH_2$ is 20.1 % and selectivity to trifluoroethylene is 99 % at 430 °C during 100 h.**

Trifluoroethylene ($CF_2$=CHF) is used as the important fluorine-containing monomer and biologically active compounds[1], which is generated through hydrodechlorination of trichlorotrifluoroethane or chlorotrifluoroethene by using the supported Pd or Ru catalyst[2-5] etc. Nevertheless, there are many difficulties in separation and purification, expensive raw and noble metal catalysts. Comparatively, dehydrofluorination of 1, 1, 1, 2-tetrafluoroethane ($CF_3CFH_2$) to synthesize trifluoroethylene is a promising route. The raw $CF_3CFH_2$ has been replaced eventually by the 2, 3, 3, 3-tetrafluoropropene due to its high Global Warming Potential (over 1300) as a new greenhouse gas[6-7]. The transformation of $CF_3CFH_2$ to trifluoro-ethylene with high additional value, resolved the excess capacity of $CF_3CFH_2$. Admittedly, it is the atomic efficiency, and has the better prospect in industrial application. However, the works about catalytic dehydrofluorination of $CF_3CFH_2$ was hardly reported in the form of professional research paper, and most of the presented works limited to the form of patents[8-10].

Dehydrofluorination of hydrofluorocarbons (HFCs) is thermo-dynamically and kinetically hindered[11-12]. To obtain a considerable yield of fluorinated olefin, it is necessary to develop highly efficient catalysts to accelerate the reaction rate. As claimed in the literature, $Mg_2P_2O_7$[13-14], $AlF_3$[15], $Fe_2O_3$-CdO-$Al_2O_3$[16] and Pd/$AlF_3$[17] catalysts were adopted for HFCs dehydrofluorination. On the other hand, the NiO/$Al_2O_3$ catalysts were applied industrially for methanation[18-19], steam reforming and pre-reforming of natural gas[20]. However, the NiO/$Al_2O_3$ catalysts used for dehydrofluorination of HFCs have not been reported scientifically.

It was disclosed that the catalytic performance of dehydro-halogenation was closely related to Lewis acidity[13-15, 21]. Teinz et al reported the dehydrohalogenation of 3-chloro-1, 1, 1, 3-tetrafluorobutane ($CF_3CH_2CFClCH_3$) over metal fluoride, and dehydrofluorination was selectively catalyzed by strong Lewis acid sites. For the dehydrofluorination of $CF_3CH_3$, the influence of strength of Lewis acid sites on formation of $CF_2$=$CH_2$ was investigated by Li et al[13-14], and Okazaki et al[15] thought that the product distribution was dependent on the acidic strength of catalysts. However, the relationships between the Lewis acid sites and activity for dehydrofluorination of $CF_3CFH_2$ are not clarified up to now.

Herein, the NiO/$Al_2O_3$ catalysts activated by HF pretreatment, were prepared for dehydrofluorination of $CF_3CFH_2$ to synthesize trifluoroethylene. Besides, the catalyst preparation, including its reaction conditions, was optimized. XRD, BET, SEM/EDX, TEM, py-IR and $NH_3$-TPD were employed to disclose the relationship between the catalyst structure and its activity. Moreover, the deactivation and regeneration of catalyst were investigated.

Table 1 Catalytic performance of fluorinated catalysts for dehydrofluorination of $CF_3CFH_2$*.

| Classification | Catalyst | Trifluoroethylene yields / % | | | | |
|---|---|---|---|---|---|---|
| | | 500 °C | 475 °C | 450 °C | 425 °C | 400 °C |
| Parent | $Al_2O_3$ | 40.7 | 36.4 | 23.2 | 16.5 | 9.8 |
| Transition | NiO/$Al_2O_3$ | 60.3 | 43.6 | 32.2 | 22.9 | 14.4 |
| | $Cr_2O_3$/$Al_2O_3$ | 37.6 | 34.3 | 29.2 | 21.9 | 14.0 |
| | PdO/$Al_2O_3$ | 26.3 | 28.4 | 20.9 | 14.4 | 9.7 |
| | $Fe_2O_3$/$Al_2O_3$ | 15.6 | 9.5 | 6.0 | 3.8 | 2.3 |
| Rare-earth | $Ce_2O_3$/$Al_2O_3$ | 48.4 | 35.8 | 26.0 | 17.8 | 11.5 |
| | $La_2O_3$/$Al_2O_3$ | 27.5 | 20.7 | 15.4 | 10.9 | 7.7 |
| Alkaline-earth | MgO/$Al_2O_3$ | 5.5 | 3.7 | 2.3 | 1.4 | 1.0 |
| | CaO/$Al_2O_3$ | 3.5 | 2.5 | 1.7 | 1.0 | 0.6 |
| | SrO/$Al_2O_3$ | 2.9 | 2.1 | 1.4 | 0.9 | 0.5 |

* Total flow = 22.5 ml $min^{-1}$, $N_2/CF_3CFH_2$ = 10, P = 1 atm, molar ratio of Al/M = 9, catalysts: 1.0 g.

γ-$Al_2O_3$ was modified by a series of metal oxides such as alkalis, alkaline earth, rare-earth, and transition metal. The oxide catalysts activated by the pre-fluorination of HF gas, were used for dehydrofluorination of $CF_3CFH_2$ to synthesize trifluoroethylene under the same reaction conditions. The trifluoroethylene yields for fluorinated $MOx/Al_2O_3$ catalysts are summarized in Table 1. The selectivity to trifluoroethylene for all catalysts is up to 99 %, and the other few byproducts are $CF_2HCF_3$ and $CF_2HCFH_2$. From Table 1, the activities of the $NiO/Al_2O_3$ and $Ce_2O_3/Al_2O_3$ are superior to the parent $\gamma$-$Al_2O_3$, and the $Cr_2O_3/Al_2O_3$ catalyst showed high activity at low temperature range of 400—450 °C. However, the $Cr_2O_3$ and the related species as a dopant in catalyst are toxic to environment and human health. The most of the transition and rare-earth metal added in the $Al_2O_3$ could not enhance its activity, and the activity of catalysts with alkaline-earth and alkalis was drastically low. Comparatively, the $NiO/Al_2O_3$ catalyst shows the environment friendly and the high catalytic activity.

We modified the $Al_2O_3$ with nickel nitrate and investigated the effect of NiO loading on its activity (Fig. S1). It was observed from the Fig. S1 (Supporting information) that with increasing NiO loading from 0 to 25 wt.%, the activity of NiAlF-12.8 catalyst reached the highest, then decreased with further increasing NiO contents over 12.8 wt.%. Moreover, activity of the NiAlF-16.7 and NiAlF-25 catalyst was lower than the parent $Al_2O_3$ (NiAlF-0). This indicated that modification of the appropriate Ni species could enhance the catalyst activity.

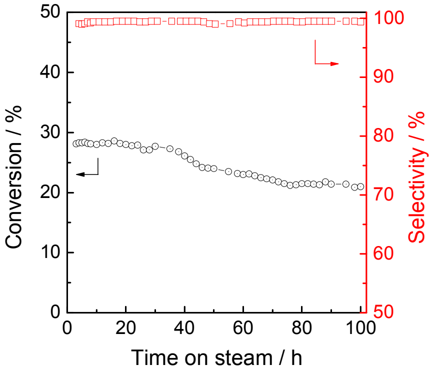

Fig. 1 The stability of NiAlF-12.8 catalyst at 430 °C

The stability test was carried out over the optimal NiAlF-12.8 catalyst at 430 °C (Fig. 1). With GHSV of 675 $h^{-1}$ and $CF_3CFH_2/N_2$ molar ratio of 10, the conversion of $CF_3CFH_2$ decreased slowly, then kept over 20.0 %. But trifluoroethylene selectivity doesn't change obviously during the on-stream time of 100 h. The activity of NiAlF-12.8 nearly kept stable after 78 h, showing a good stability at a proper reaction temperature.

The deactivation of NiAlF-12.8 catalyst was accelerated in the dehydrofluorination process under the conditions of high temperature, high GHSV and low ratio of $N_2$ to $CF_3CFH_2$. The regeneration of deactivated NiAlF-12.8 catalyst was performed by a temperature-programmed calcination with a rising rate of 2 °C/min to 550 °C for 2 h in the mixed flow nitrogen of containing 10% oxygen. The regenerated NiAlF-12.8 catalyst needs to be pre-fluorinated again before reaction. The results are listed in Table S1. It was found that the reactivity could be recovered by more than 94 % of the fresh catalyst, indicating that NiAlF-12.8 catalyst has an excellent regeneration capability.

Fig. 2 shows the XRD patterns of a) NiAlO and b) NiAlF catalysts. From Fig. 2 a), the diffraction peaks of $Al_2O_3$ phase were observed for all NiAlO catalyst. No diffraction peaks due to NiO phase are observed for the NiAlO-6 and NiAlO-12.8 catalysts[22]. With increasing NiO content, the intensity of NiO diffraction peaks appeared and got stronger, whereas the $Al_2O_3$ diffraction peaks weaken. For the NiAlO-25 catalyst, the peaks with strong intensity were attributed to the bulk NiO crystalline[23]. After prefluorination of NiAlO catalysts, the characteristic peaks due to $AlF_3$ and $NiF_2$ phase are shown in Fig. 2b). The intensity of diffraction peaks of $AlF_3$ at 25.3 ° due to (012) plane, firstly increased, then reached up to the maximum with the 12.8% of NiO content. The low content of Ni species could accelerate the crystal growth of $AlF_3$ crystalline particle under the fluorination, causing the intensity of $AlF_3$ peak initially to increase. In addition, the $NiF_2$ diffraction peaks got stronger gradually. It was indicated that the extended exposure of $NiO/Al_2O_3$ catalyst to fluorinating gases at elevated temperature, lead to complete conversion of $Al_2O_3$ and NiO to $AlF_3$ and $NiF_2$, respectively.

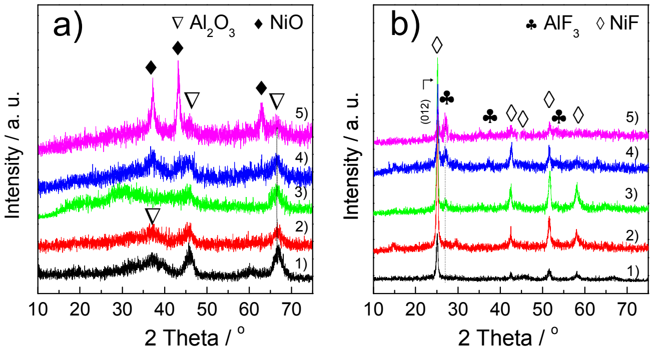

Fig. 2 XRD patterns of a) NiAlO and b) NiAlF catalysts. The NiO loading is 1) 0 %, 2) 6.0 %, 3) 12.8 %, 4) 16.7 %, 5) 25.0 %.

$N_2$ adsorption isotherms and pore size distributions of NiAlF catalysts are shown in Fig. S2. All isotherms are type IV according to the IUPAC classification. Other parameters, such as surface area, pore volume, and pore size, are summarized in Table S2. There is an increase of the surface area with the amount of nickel (from 0 to 12.8 wt%). Fig. S3 shows the SEM images of catalysts. The NiAlO-12.8 catalyst is disordered in Fig. S3 a, most of the bulk grains are the crystalline $AlF_3$ formed by fluorination in Fig. S3 b.

Firstly, the acidic amount and strength of NiAlF catalysts were measured using $NH_3$-TPD techniques. Fig. 3 shows $NH_3$-TPD profiles of NiAlF catalysts with different NiO loading. The acidic amount was also calculated and listed in Fig. 3 (inserted). The broad peaks around 170 °C and 315 °C could be ascribed to the $NH_3$ adsorbed on the weak acidic sites and strong acidic sites[24], respectively. With increasing content of Ni species, the acidic amount increases, then declines drastically, and reaches the maximum for the NiAlF-12.8. The acidic amount of NiAlF-12.8 (0.43 mmol $g^{-1}$) and NiAlF-6 catalyst (0.37 mmol $g^{-1}$) is larger than NiAlF-0 ($AlF_3$, 0.34 mmol $g^{-1}$) catalyst. However, the NiAlF catalysts with high Ni species loading (>12.8 wt.%) show the weak acidity.

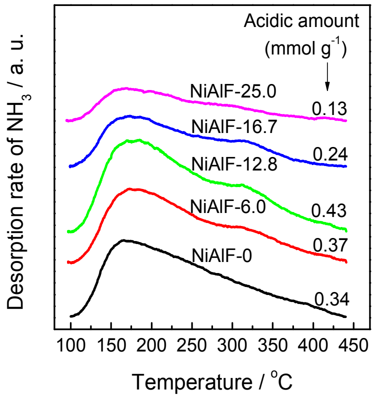

Fig. 3 $NH_3$-TPD profiles of NiAlF catalysts.

Pyridine adsorption experiments were conducted to determinate the properties of acidic sites. Obviously, two characteristic bands at $v_{19b}$=1448 and $v_{8a}$=1612 cm$^{-1}$ due to the Lewis acid sites[25-26] on $AlF_3$ catalysts are observed in Fig. 4 a). For the NiAlF-12.8 catalyst, the $v_{8a}$ feature includes 1622 and 1616 cm$^{-1}$, associated with the strong and weak Lewis acid sites[27-28], respectively. But the catalyst without Ni additive (NiAlF-0), has only one type of Lewis acid at 1612 cm$^{-1}$. That indicates the $NiF_2$ plays an important role on acidity of NiAlF catalyst. The NiAlF-12.8 catalyst adsorbed pyridine at room temperature, were outgassed at 100 or 300 °C, their py-IR spectra shown in Fig. 4b). The bands shift were observed, with increasing the desorption temperature on NiAlF-12.8 catalyst in Fig. 4b). This shift with temperature shows the higher strength of acidity. M. Wojciechowska et al[24] reported that new Lewis acid sites appeared on the surface of $MgF_2$ catalyst doped appropriate $NiF_2$, which originated from the coordinatively unsaturated $Ni^{2+}$ ions. These facts agreed with our findings in which that the new Lewis acid sites presented in the $NiF_2/AlF_3$ catalyst (Fig. 3). It is considered that the Ni content plays an important role on the number of acid sites on the NiAlF catalyst.

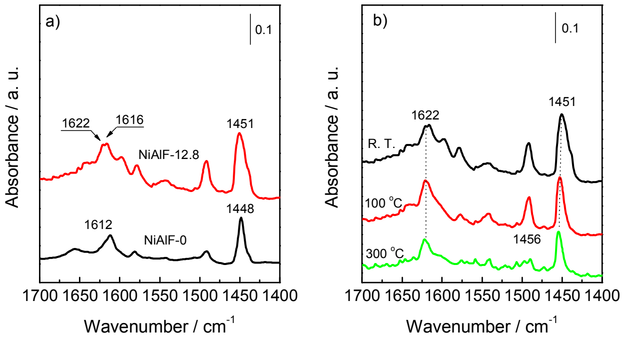

Fig. 4 Infrared spectra of adsorbed pyridine for catalysts.

Halbert group et al[29-30] reported the cleavage of C-F in dehydrofluorination of $CF_3CH_3$ and $CF_2HCH_3$. In general, C-F cleavage (dissociation energy is 522.0 ± 8.4 kJ mol$^{-1}$) needs a high activation energy, companying with high reaction temperature. It is well known that the Lewis acid sites are considered to activate C-F bond. Li et al[13] reported the dehydrofluorination of $CF_3CH_3$ into $CF_2H_2$ over Lewis acidic $Mg_2P_2O_7$ catalyst. Teinz et al[21] reported that C-F bond activation over Lewis acid sites was the initial step of dehydrohalogenation. Therefore, Lewis acid sites play a key role in the dehydrofluorination of $CF_3CFH_2$. Fig. 5 shows the relationship between Lewis acid sites and the activity of the NiAlF catalysts. It is interestingly found that the number of Lewis acid sites is closely proportional to conversion of $CF_3CFH_2$ (Fig. 5). NiAlF-12.8 catalyst behaved the high activity, attributed to its large Lewis acidic amount. In conclusion, it is undoubtedly suggested that Lewis active sites were mainly the active sites of catalysts for dehydrofluorination of $CF_3CFH_2$.

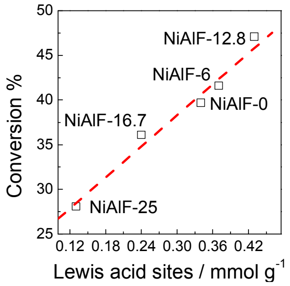

Fig. 5 Dependence of amount of Lewis acid sites on the conversion of $CF_3CFH_2$, $N_2/CF_3CFH_2$ = 10, P = 1 atm, catalyst: 1.0 g.

According to thermodynamics parameter of $CF_3CFH_2$ dehydrofluorination reaction[11] [$\Delta_r G^0$ (298K) = 70.3 kJ mol$^{-1}$; $\Delta_r H^0$ (298K) = 128.6 kJ mol$^{-1}$], this reaction favors a high temperature. The influence of temperature from 375 to 530 °C on NiAlF catalyst was showed in Fig. S4. With elevating the reaction temperature, the selectivity to trifluoroethylene decreased from 100 to 96.8%, accompanied with the formation of CFH=CFH, $CF_2HCF_3$ and $CF_2HCFH_2$. The byproducts derived from pyrolysis and isomerization[31-32] of $CF_3CFH_2$ at high temperature. When dehydrofluorination of $CF_3CFH_2$ was conducted at high temperature (≥480 °C), the used catalysts turned into black in a short time, indicating that the serious coke or polymerization occurred over the catalysts. Therefore, a proper reaction temperature should be selected in the range of 400—480 °C.

As can be seen from the Fig. 1, the deactivation behavior of the catalysts was investigated. Fig. S5 shows the XRD patterns of the used NiAlF-5 catalyst with different reaction time. Only the $AlF_3$ and $NiF_2$ phase was observed in the NiAlF-5 catalyst for 100 h, and the peak intensity increased with time on steam. It is indicated that the crystalline size of $AlF_3$ and $NiF_2$ increased with the reaction time on steam, and the catalyst was slowly sintered. Fig. S6 shows the Raman spectra of the used NiAlF-12.8 catalyst for different reaction time. Other intense broad bands located at 1318 and 1593 cm$^{-1}$ in the Raman spectra are attributed to the A1g vibration mode and the $E_{2g}$ vibration mode of the carbon[33], respectively. The intensity of Raman peak due to carbon species increased with reaction time, demonstrating that the level of formed coke became higher and higher with the time on steam.

TG experiments were conducted to further illustrate the coke for the deactivated NiAlF-12.8 catalyst during the reaction process, shown in Fig. S7. An obvious weight loss was observed below 100 ◦C in all used NiAlF-12.8 catalysts, attributed to the loss of physical adsorption $H_2O$. In addition, a main weight loss was observed around the broad range from 500—590 ◦C, undisputedly, assigned to the combustion of deposited carbon on used NiAlF catalysts[34]. It is found that the weight loss of used catalysts increase with the reaction time on steam. It is further confirmed that the coke result in the decline of catalyst activity, in agreement with the results by Raman (Fig. S6). It can be implied that the deactivation mainly depends on the sintering and carbon deposition over the catalyst.

In summary, the fluorinated $NiO/Al_2O_3$ catalyst was developed for a promising process on the catalytic dehydrofluorination of $CF_3CFH_2$ to synthesize trifluoroethylene. The optimized NiAlF catalyst with 12.8 wt% NiO shows an excellent performance, giving 20% conversion and 99% selectivity with a good stability. It is found that the number of Lewis acid sites and activity of the NiAlF catalysts is closely linear regression relation. In addition, the slow deactivation is mainly attributed to coke deposition over the catalyst, and the deactivated catalyst can be easily regenerated by heating at 550 °C. More importantly, the fluorinated $NiO/Al_2O_3$ catalyst with the excellent defluorination performance, could be applied to other dehydrofluorination of HFCs, such as dehydrofluorination of $CF_2HCH_3$ (HFC-152a) to synthesize vinyl fluoride (a very important fluoride monomer).

## Acknowledgement

This work was financially supported by CNPC Inovation Research Funds (2012D-5006-0505) and National Natural Science Foundation of China (51174277 and 20873091).

## Notes and references

*a Department of Chemistry, Tongji University, Shanghai 200092, China. Fax: (+86) 21-65982563; E-mail: zhuzhirong@tongji.edu.cn.*

† *Electronic Supplementary Information (ESI) available: [details of any supplementary information available should be included here]. See DOI: 10.1039/c000000x/*

1 T. Saiki, M. Sumida, S. Nakano, K. Murakami. Method for producing trifluoroethylene, US patent 5283379 (1994).

2 B. C. Meng, Z. Y. Sun, J. P. Ma, G. P. Cao, W. K. Yuan, *Catal. Lett.*, 2010, **138**, 68.

3 R. Ohnishi, W. L. Wang, M. Ichikawa, A*ppl. Catal., A*, 1994, **113**, 29.

4 S. P. Scott, M. Sweetman, J. Thomson, A. G. Fitzgerald, E. J. Sturrocky, *J. Catal.*, 1997, **168**, 501.

5 T. Mori, T. Yasuoka, Y. Morikawa, *Catal. Today*, 2004, **88**, 111.

6 K. P. Shine, W. T. Sturges, *Science*, 2007, **315**, 1804–1805.

7 S. Henne, D. E. Shallcross, S. Reimann, P. Xiao, D. Brunner, S. O'Doherty, B. Buchmann, *Environ. Sci. Technol.*, 2012, **46**, 1650.

8 H. Serge, L Andre, FR patent 2710054 (1995).

9 H. Serge, FR patent 2729136 (1997).

10 R. Powell, A. Sharratt, US patent 5856593 (1999).

11 A. W. Baker, D. Bonniface, T. M. Klapotke, I. Nicol, J. D. Scott, W. D. S. Scott, R. R. Spence, M. J. Watson, G. Webb, J. M. Winfield, *J. Fluorine Chem.*, 2000, **102**, 279.

12 A. Kohne, E. Kemnitz, *J. Fluorine Chem.*, 1995, **75**, 103.

13 G. L. Li, H. Nishiguchi, T. Ishihara, Y. Moro-oka, Y. Takita, *Appl. Catal., B*, 1998, **16**, 309.

14 G. L. Li, T. Ishihara, H. Nishiguchi, Y. Moro-oka, Y. Takita, *Chem. Lett.*, 1996, **7**, 507.

15 S. Okazaki, S. Toyota, *Nikkashi* 1972, 1615.

16 T. S. Sirlibaev, A. Akramkhodzhaev, K. U. Usmanov, *J. Appl. Chem. USSR*, 1985, **58,** 1541.

17 M. Tojo, S. Fukuoka, H. Tsukube, *Bull. Chem. Soc. Japan.*, 2011, **84**, 333.

18 J. R. Røstrup-Nielsen, K. Pedersen, J. Sehested, *Appl. Catal., A*, 2007, **330**, 134.

19 J. Kopyscinski, T. J. Schildhauer, S. M. A. Biollaz, *Fuel*, 2010, **89**, 1763.

20 J. Sehested, *Catal. Today*, 2006, **111**, 103.

21 K. Teinz, S. Wuttke, F. Börno, J. Eicher, E. Kemnitz, *J. Catal.*, 2011, **282**, 175; J. Thomson, G. Webb, J. M. Winfield, *J. Molecular Catal.*, 1991, **68**, 347.

22 M. Blanchard, J. Barrault, A. Derouault, *Studies in Surface Science and Catalysis*, 1991, **63**, 687.

23 G. Garbarino, I. Valsamakis, P. Riani, G. Busca, *Catal. Commun.*, 2014, **51**, 37.

24 M. Wojciechowska, S. tomnicki, M. Pietrowski, *J. Fluorine Chem.*, 1996, **76**, 133.

25 G. Ramis, L. Yi, G. Busca, *Catal. Today*, 1996, **28**, 373.

26 G. Busca, *Phys. Chem. Chem. Phys.*, 1999, **1**, 723.

27 John M. Winfield, *J. Fluorine Chem.* 2009, **130**, 1069.

28 M. Moreno, A. Rosas, J. Alcaraz, M. Hernández, S. Toppi, P. Ds Costa, *Appl. Catal., A*, 2003, **251**, 369.

29 B. D. Neely, H. Carmichael, *J. Phys. Chem.*, 1973, **77**, 307.

30 B. Noble, H. Carmichael, C. L. Bumgardner, *J. Phys. Chem.*, 1972, **76**, 1680.

31 E. Kemnitz, K. U. Niedersen. *J. Catal.*, 1995, **155**, 283.

32 K. U. Niedersen, E. Schreier, E. Kemnitz, *J. Catal.*, 1997, **167,** 210.

33 Y. Xia, W. K. Zhang, Z. Xiao, H. Huang, H. J. Zeng, X. R. Chen, F. Chen, Y. P. Gan, X. Y. Tao, *J. Mater. Chem.*, 2012, **22**, 9209.

34 Y. Kobayashi, J. Horiguchi, S. Kobayashi, Y. Yamazaki, K. Omata, D. Nagao, M. Konno, M. Yamada, *Appl. Catal., A*, 2011, **395**, 129.